[69]N. W. Ashcroft and D. C. Langreth, Phys. Rev. 155, 682 (1967).
[70]E. J. Woll and W. Kohn, Phys. Rev. 126, 1693 (1962).
[71]G. Björkman, B. I. Lundquist, and A. Sjölander, Phys. Rev. 159, 551 (1967).
[72]T. D. Schultz, *Quantum Field Theory and the Many-Body Problem* (Gordon and Breach, New York, 1964), p. 96.

PHYSICAL REVIEW B VOLUME 3, NUMBER 12 15 JUNE 1971

Study of Thermal Diffuse X-Ray Scattering from Lead Single Crystals*†

Sanford L. Schuster
Physics Department, Mankato State College, Mankato, Minnesota 56001

and

John W. Weymouth
Behlen Laboratory of Physics, University of Nebraska, Lincoln, Nebraska 68508

(Received 21 September 1970)

Thermal diffuse x-ray scattering (TDS) from lead single crystals has been measured in the longitudinal and transverse branches along the [100] and [111] directions. In order to determine if one can use x rays to obtain reliable dispersion curves from a metal such as lead, the measured TDS was compared with that calculated from lead dispersion curves obtained by means of slow-neutron scattering. The one-phonon intensity was calculated directly from the [100] and [111] neutron data, and the two-phonon intensity was calculated by a method which expresses the cross section in terms of the atomic force constants determined by a fit to the neutron data. The intensity of the higher-order scattering was calculated by a method in which the Debye-Jauncey relation for TDS is expanded in powers of the Debye-Waller factor and the first two terms are subtracted. In addition, a very small Compton-scattering contribution was calculated. It is observed that in all cases, except for some points along the [111] transverse branch, the measured intensity is greater. The differences range from 10 to 60% or higher, and have a periodic dependence on reciprocal-lattice position. The source of this extra scattering has not yet been conclusively identified.

I. INTRODUCTION

In this paper we present the results of a study of thermal diffuse x-ray scattering (TDS) from lead single crystals along the [100] and [111] directions. The intensity of this scattering is compared with the expected intensity calculated from lead phonon dispersion curves determined by means of slow-neutron scattering.[1,2] This study was initiated in order to examine the extent to which x rays, as distinct from neutrons, can be used to obtain reliable phonon dispersion curves in a metal such as lead. The approach was to make a careful examination of the validity of the multiphonon corrections to experimentally obtained TDS data.

TDS provides an indirect approach to the determination of dispersion relations, since the dispersion relations are determined from the intensity of the total x-ray scattering. The total scattering includes not only photon–single-phonon scattering events, but also photon–multiple-phonon scattering events and Compton scattering. On the other hand,

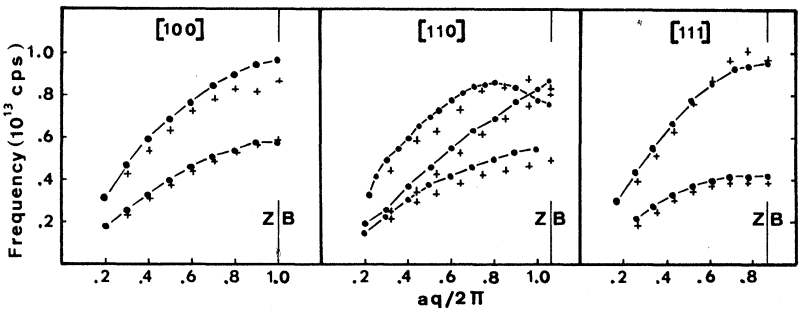

FIG. 1. Aluminum dispersion curves. -·-·-·-, neutron results from Ref. 9. +, x-ray results from Ref. 7.

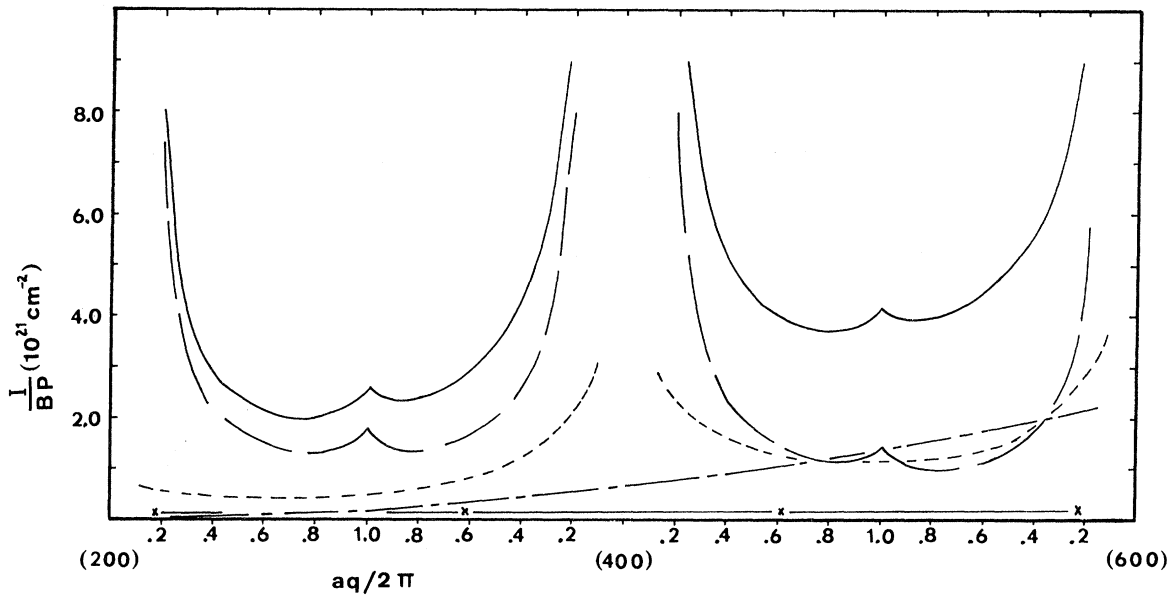

FIG. 2. Calculations corresponding to [100] longitudinal TDS. ——, total. —— ——, first order. -------, second order. —— — —— —, higher orders. x ————x, Compton. I is the calculated intensity, B is the constant determined by the apparatus divergences, and P is the polarization factor.

the inelastic scattering of slow neutrons provides a direct means of determining dispersion relations, since the measurable energy change of a neutron in a neutron-phonon scattering process immediately gives the frequency of a lattice vibration.

Past investigations in which x rays have been used to determine dispersion relations in metals[3–8] yield curves which generally fall below the corresponding curves determined by means of neutron scattering. Figure 1 displays the dispersion relations for aluminum as determined by both neutrons[9] and x rays.[7] The frequencies are plotted against the reduced dimensionless wave vector $aq/2\pi$, where a is the lattice constant and q is the wave-vector magnitude associated with a vibrational state. The differences in the results of the two approaches most likely occur because of the difficulties inherent in extracting the frequencies from the x-ray data. Accurate calculations of the Compton scattering are available for this purpose,[10] but if the multiple-phonon contributions are to be accounted for, it is necessary that one assume a form for the dispersion relations in order to calculate such contributions. The approximations used for the curves have not been very good for metals. In addition, one must be sure that the data is correctly normalized, and that the effects of any surface contamination of the samples are taken into account.

Although it has a high absorption coefficient, lead was chosen as the metal to be examined, since, as is shown in Figs. 2–5, the first-order scattering does not dominate the higher orders in the regions of reciprocal space investigated. Thus, good calculations of the higher orders are required if the intensity expected from calculations is to be compared with the measured intensity of the x-ray scattering. Since the second-order scattering is

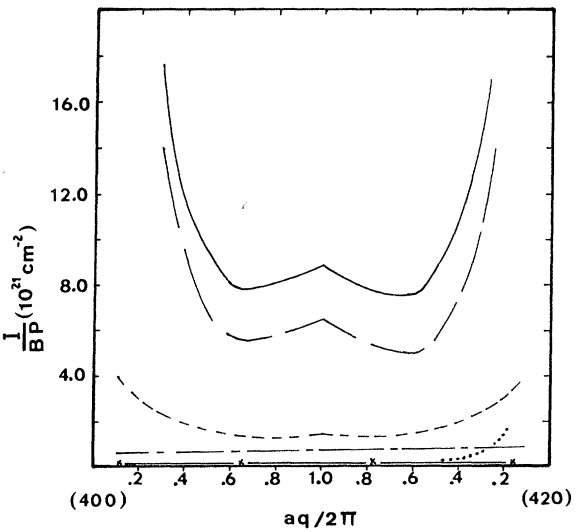

FIG. 3. Calculations corresponding to [100] transverse TDS. ——, total. —— ——, first-order transverse. · · · · ·, first-order longitudinal. -----, second order. —— — —— —, higher orders. x————x, Compton. I is the calculated intensity, B is the constant determined by the apparatus divergences, and P is the polarization factor.

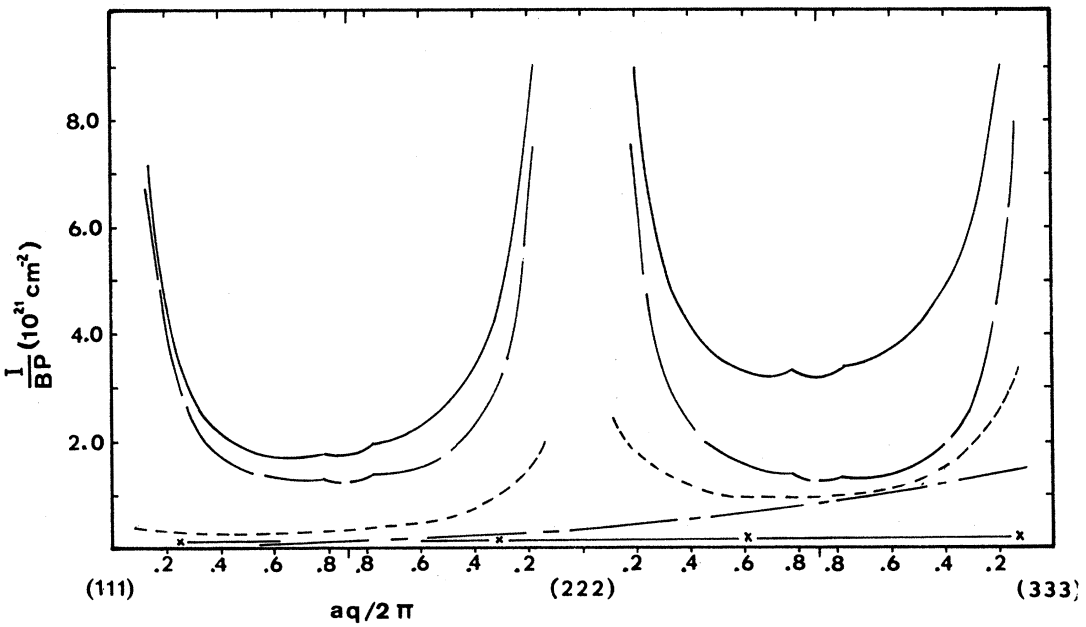

FIG. 4. Calculations corresponding to [111] longitudinal TDS. ——, total. ——— ———, first order. -------, second order. —— — —— —, higher orders. x————x, Compton. I is the calculated intensity, B is the constant determined by the apparatus divergences, and P is the polarization factor.

calculated by use of the neutron results, any large disagreement between the measured scattering and that calculated cannot be attributed to the second-order calculation.

In Sec. II, the cross sections for the various contributions to the scattering are given, while Sec. III describes the experimental procedure. In Sec. IV, the experimental measurements are compared with the calculations, and Sec. V is devoted to a discussion of the observed differences.

II. THEORY AND CALCULATIONS

A. One-Phonon Cross Section

The contribution to the TDS from photon–single-phonon scattering events, in counts/sec, is given by[11]

$$I_1 = \frac{BPf^2 e^{-2M}}{2(\mu/\rho)m^2}\left(\sum_j \frac{(\vec{S}\cdot\vec{e}_{\vec{q}j})^2\langle E_{\vec{q}j}\rangle_{av}}{\omega^2_{\vec{q}j}}\right)_{\vec{S}+\vec{q}=\vec{\tau}}, \quad (1)$$

where P is $(1+k\cos^2 2\theta)/(1+k)$, the polarization factor, k is the ratio of the incident intensity associated with a polarization parallel to the diffraction plane to that associated with a polarization perpendicular to the diffraction plane, B, which has units of cm^2/sec, is the constant determined by the apparatus divergences, μ/ρ is the mass-absorption coefficient, m is the atomic mass, f is the atomic-scattering factor, e^{-2M} is the Debye-Waller factor, $\vec{S}$ is the diffraction vector, $\omega_{\vec{q}j}$ is the angular frequency of the vibrational mode specified by the wave vector $\vec{q}$ and polarization state j, $\langle E_{\vec{q}j}\rangle_{av}$ is the

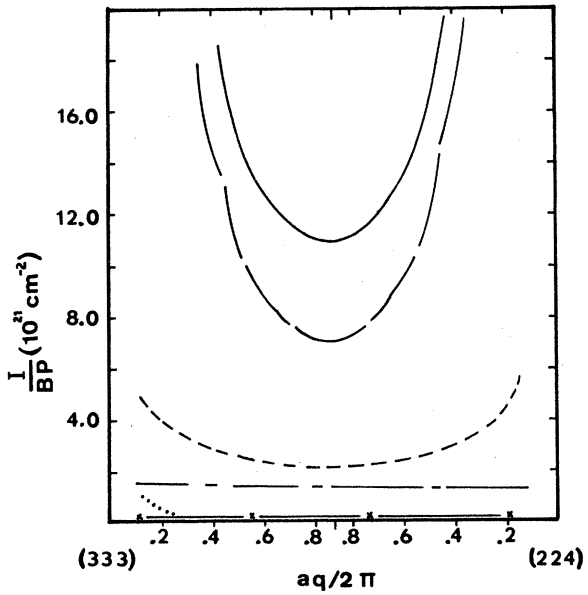

FIG. 5. Calculations corresponding to [111] transverse TDS. ——, total. ——— ———, first-order transverse. · · · · ·, first-order longitudinal. ----, second order. ——— – ——— —, higher orders. x————x, Compton. I is the calculated intensity, B is the constant determined by the apparatus divergences, and P is the polarization factor.

average energy of the $\vec{q}j$ mode, $\vec{e}_{\vec{q}j}$ is the polarization vector of the $\vec{q}j$ mode, and $\vec{\tau}$ is a reciprocal-lattice vector.

In the calculation of I_1 the frequencies used were those due to Brockhouse *et al.*,[1] but corrected to room temperature. The corrections were made by using differences in the 100 and 296 °K interplanar force constants, as reported by Brockhouse *et al.* in an earlier work.[12] These force constants were determined by making a fit of the symmetry-direction dispersion curves. The fractional changes in the force constants were then applied to the 100 °K force constants reported by Brockhouse *et al.*[1] as having been calculated from more precise dispersion-curve data. This procedure allowed the fractional changes in the more precise frequencies to be calculated for a temperature rise from 100 to 296 °K. The result was a slight reduction in the frequencies, and is in good agreement with the room-temperature results of Stedman *et al.*[2]

B. Two-Phonon Cross Section

The contribution to the TDS from photon–two-phonon scattering events was calculated according to a method outlined by Froman,[13] in which the average energy per mode is assumed to be $\kappa_B T$. This is a good assumption, since the Debye temperature of lead is about 85 °K and the data were taken at room temperature. The calculation involves an integral over the first Brillouin zone in which the integrand is expressed in terms of atomic force constants instead of polarization vectors and frequencies. The atomic force constants used were those determined by Gilat[14] for lead out to eight neighbors by making a least-squares fit of the phonon dispersion curves obtained by Brockhouse *et al.*[1] at 100 °K. With this approach the second-order contribution, in counts/sec, is given by[15]

$$I_2 = \frac{\pi B P V_c f^2 e^{-2M} (k_B T)^4}{8(\mu/\rho)m} \left(\frac{\sin\theta}{\lambda}\right)^4 \times \int R(\vec{q}, \hat{S})\, R(\vec{S} - \vec{q}, \hat{S})\, dV_{\vec{q}} \,, \quad (2)$$

where V_c is the volume per atom, λ is the x-ray wavelength, $\hat{S}$ is the unit vector in the direction of the diffraction vector, and $R(\vec{q}, \hat{S})$ is the function which contains the force constants. The integral is over the first Brillouin zone. For example, for the traversal from the (400) to the (420) reciprocal-lattice point

$$R(\vec{q}, \hat{S}) = \frac{1}{16+\eta^2}\left(\frac{16(D_{22}D_{33} - D_{23}^2) + 8\eta(D_{13}D_{23} - D_{12}D_{13}) + \eta^2(D_{11}D_{33} - D_{13}^2)}{D_{11}D_{22}D_{33} + 2D_{12}D_{13}D_{23} - D_{11}D_{23}^2 - D_{22}D_{13}^2 - D_{33}D_{12}^2}\right) , \quad (3)$$

where η is a dimensionless coordinate along (400) to (420), and the $D_{\alpha\beta}$ are given by Squires.[16]

C. Higher-Order Cross Section

The higher-order TDS, which consists of photon–multiple-phonon scattering events above the second order, is calculated in a manner which has been used successfully by Eldridge in his x-ray investigation of sodium chloride[17] and later of cesium iodide.[18] The method is one in which the Debye-Jauncey expression for TDS[19] is expanded in powers of the Debye-Waller factor and the first two terms are subtracted. As Eldridge has shown,[17] this leaves only the higher-order scattering contributions, for which the Debye-Jauncey expression should be a good approximation. This is true, since the TDS maxima which do occur are due primarily to the first-order scattering, as the first-order scattering at any $\vec{S}$ is determined by a specific $\vec{q}$. The maxima in the second-order scattering are much less pronounced, since at any $\vec{S}$ the second order is due to contributions from many pairs of $\vec{q}$'s. The higher-order scattering terms involve contributions from even many more combinations of wave vectors, with the result that the tendency of any single combination to cause a peaking is washed out. The expression used for the higher-order scattering, in counts/sec, is

$$I_h = \frac{BPf^2 e^{-2M}}{2(\mu/\rho)m} \left(e^{2M} - 1 - 2M - 2M^2\right) . \quad (4)$$

Equation (4) does not allow for a small peaking which should occur near reciprocal-lattice points.

D. Compton Cross Section

The Compton scattering, in counts/sec, was calculated by use of

$$I_c = \frac{BPi_c(\vec{S})}{[(\mu/\rho) + (\mu'/\rho)]m} \,, \quad (5)$$

where μ'/ρ is the mass-absorption coefficient for the radiation scattered at an angle 2θ, and for lead $i_c(\vec{S})$ is the expression for the Compton scattering, in electron units, due to Heisenberg.[20] This approach is based upon the Thomas-Fermi atomic model and is applicable to the heavy atoms.

E. Calculations

The results of the calculations are shown in Figs. 2–5. It can be seen that the second- and higher-order contributions are especially important between the (222) and (333), and the (400) and (600)

reciprocal-lattice points. The higher-order contribution should show some peaking at reciprocal-lattice points, but it does not because of the nature of the calculation.

The atomic scattering factor used in the calculations is that due to Cromer and Waber,[21] with dispersion corrections due to Cromer.[22] The Debye-Waller factor used corresponded to the Debye temperature of 85 °K measured by Alexopoulous *et al.*[23]

III. EXPERIMENT

A. Samples

Lead of 99.999% purity was used to grow several lead crystals from the melt. The [111] and [100] oriented crystals chosen for the study were each found to have a rocking-curve half-width of about 12 min. The procedure adopted in order to reduce the surface contamination as much as possible consisted of several steps. Each sample was first polished for 5 min in an etch consisting of three parts glacial acetic acid and one part 30% hydrogen peroxide. A second polish was carried out for 10 min in an etch consisting of six parts glacial acetic acid, one part 30% hydrogen peroxide, and one part distilled water. The polishing process was followed by a rinse in distilled water in order to remove the etching solution, and then by a vigorous rinse in kerosene in order to replace the water layer with a kerosene layer. The kerosene protected the sample from oxidation during transfer from the acid polisher to a sputtering chamber. Once a sample was inside the sputtering chamber the system was pumped down in order to remove the kerosene surface layer. The sample was then ion bombarded with argon ions and carbon sputtered. In a very striking manner this procedure removed some large powder peaks which had been showing up in the TDS.

B. Apparatus and Procedure

A Picker 816 constant-potential generator and control, a Picker vertical-axis diffractometer, and a Dunlee high-intensity copper-anode x-ray tube were used in this work. The tube was normally operated at 40 kV and 24 mA. The x-ray beam was very stable, as the only variations were of the order of hours and due to variations in room temperature and atmospheric pressure.

A premonochromator was used to monochromatize the incident x-ray beam. This monochromator, which includes a rotatable x-ray tube mount, was designed by one of us and is described in detail in the thesis[24] on which this article is based. The monochromator utilizes a lithium fluoride crystal doubly bent into a form described by Warren[25] and Chipman[26] in order to reduce the vertical divergence in the incident beam. Since the x-ray tube was normally operated at 40 kV, the monochromator passed the second, third, and fourth multiples of the 8.05-keV Cu $K\alpha$ line. The half-wavelength contribution turned out to be the only important one, but, as discussed below, its effect was negated in those reciprocal-space regions where it was troublesome by reducing the tube voltage to 14 kV.

The goniostat which was used is a copy of that described by Costello.[27] The samples were mounted in a vacuum chamber attached to the goniostat. The vacuum-chamber window, which was about 2 in. from the sample, was a piece of 0.5-mil Mylar glued with epoxy onto the brass surface of the chamber. During this work the vacuum was maintained in the range from about 100 to 300 μ.

The detector used was a xenon-filled proportional counter and preamplifier assembly supplied by Picker. The output was sent through a linear amplifier to a pulse-height analyzer (PHA) whose window was set wide enough so that it encompassed the 8.05-keV Cu $K\alpha$ peak and allowed for some drift of the peak. It was found that the Picker detector had some half-wavelength contamination in the window settings employed. This was due to iron fluorescence from the back wall of the counter tube. In regions where it became important, the half-wavelength contamination was eliminated by running the x-ray tube at 14 kV and 32 mA, and then normalizing the data to that obtained at 40 kV and 24 mA.

The output of the PHA was fed into a 128-channel analyzer (MCA) operated in the multiscaling mode. This system allowed the collection of data in such a manner that variations in the incident beam intensity which were of several hours duration had no effect on the shape of the data.[28] The detector was made to scan back and forth over selected 2θ intervals in the θ-2θ scan mode, while at the same time the MCA, operating in the multiscaling mode, acquired data corresponding to specific 2θ intervals in each of its channels. The signals which controlled the MCA were provided by switches on the diffractometer. These were tripped at such times that the multiscaling operation of the MCA was synchronized with the 2θ scanning motion of the detector. In actual operation the system was sometimes run continuously for 4 days, except for data prints taken about every 12 h of running time. The noise inherent in the entire detection system, including the analyzer, was found to be 0.16 ± 0.02 counts/sec.

The data-accumulation procedure described above was used for the [100]L and [111]L modes, for which the diffraction vector was perpendicular to the surface of the [100] or [111] oriented crystal under investigation. Data was acquired by hand when the [100]T and [111]T modes were investi-

gated, since these traversals required changes not only in 2θ, but also in ω, the sample angular motion which is independent of 2θ and in the diffraction plane.

X-ray scattering from lucite was used to determine the absolute intensity of the TDS from lead. The theoretically expected scattering for lucite, I_{LT}/BP, was calculated by use of scattering factors, Compton contributions, and mass-absorption coefficients taken from the *International Tables for X-Ray Crystallography*.[10] I_{LT}/BP was then compared with the measured scattering I_{LM} in the 2θ interval from 120° to 135°. Under the assumption that $I_{LT}=I_{LM}$, BP was determined as a function of 2θ. Since $BP=[B/(1+k)]+[Bk/(1+k)]\cos^2 2\theta$, it was expected that the BP data points plotted against $\cos^2 2\theta$ would fall along a straight line. This was found to be the case, and a least-squares fit gave $B/(1+k)$ and $Bk/(1+k)$, from which B and k were determined. The data presented here were taken with $B=2.84\times10^{-21}$ cm^2/sec and and $k=0.85$. It should be noted that this value of k is larger than that expected for either a mosaic or perfect crystal. Jennings[29] also has found such a result, but his value of k is much closer to that expected for a perfect crystal.

C. Instrumental Resolution

The resolution in reciprocal space was determined by the angular divergences allowed by a four-way adjustable slit immediately after the monochromator, the width of the beam focus at the sample, and a four-way adjustable slit just before the detector. A tube, adjustable in length, extended from the detector slit to the vacuum-chamber window in order to prevent any extraneous scattering from reaching the detector. The incident horizontal divergence was 1°35′, the incident vertical divergence was about 12′, the exit horizontal divergence was 52′, and the exit vertical divergence was 1°. These divergences were the worst possible allowed by the slit and focus sizes, but, due to structure in the incident beam, the resolution in reciprocal space was smaller than that predicted by the numbers. In terms of a reciprocal space in which the coordinates are multiplied by $a/2\pi$, the resolution ranged from 0.040 at $2\theta=46.00°$ to 0.025 at $2\theta=107.90°$ in the direction parallel to the diffraction vector. For the direction in the diffraction plane perpendicular to the diffraction vector, the resolution ranged from 0.017 to 0.036 for the same 2θ interval. These numbers were determined from the geometry of the system and include the effect of the 2θ sweep motion and channel dwell time of the MCA.

IV. RESULTS

The experimental data and relevant calculations are shown in Figs. 6–9. In each instance the count rate is plotted against $aq/2\pi$, and the reciprocal-space position is given by the coordinates of the reciprocal-lattice vectors along the direction in question. In all cases any error bars shown correspond to the fractional uncertainty interval $\pm1/N^{1/2}$, where N is the total count acquired for any particular data point. The data described as longitudinal data were acquired in such a manner that the diffraction vector lay along the appropriate

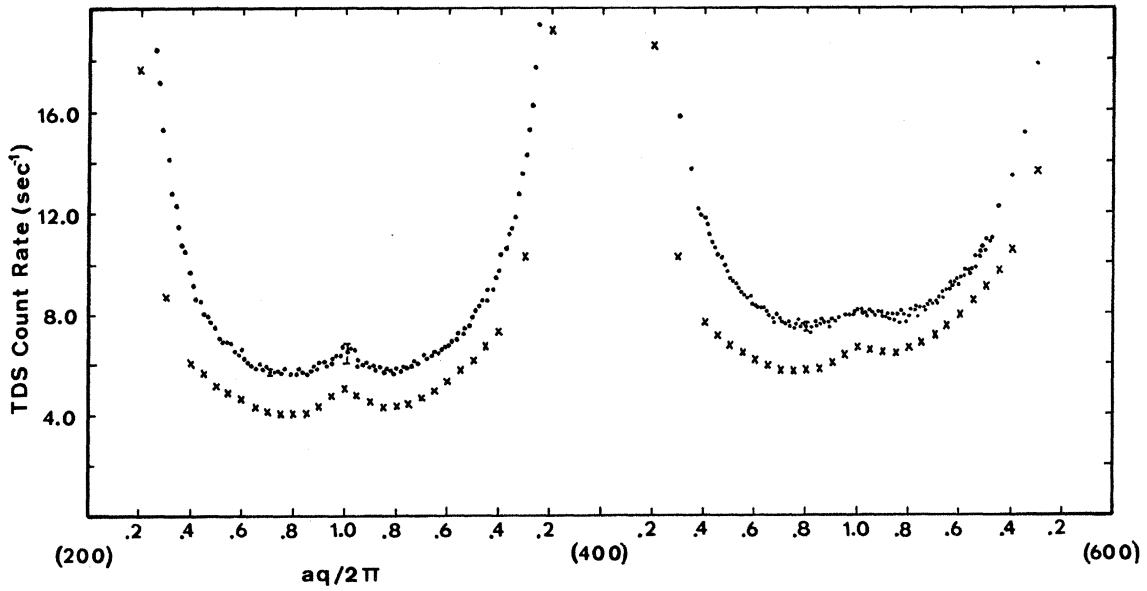

FIG. 6. Total [100] longitudinal TDS. • experimental points; × calculated points.

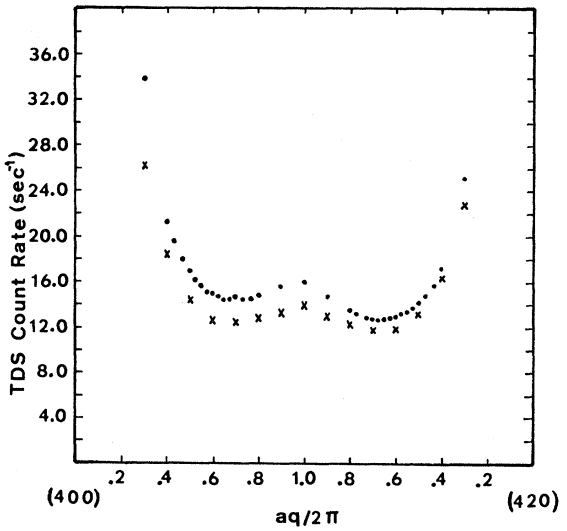

FIG. 7. Total [100] transverse TDS. • experimental points; × calculated points.

symmetry direction. Since the polarization vectors of the vibrational modes along a symmetry direction are parallel and perpendicular to the direction, Eq. (1) shows that the first-order TDS is associated with longitudinal phonons. The transverse data were acquired in a way such that the diffraction vector was kept nearly perpendicular to a symmetry direction. The first-order TDS then was associated with transverse phonons.

The transverse data shown in Figs. 7 and 9 had to undergo absorption corrections, since they were acquired by moving the crystal normal away from the diffraction vector in the diffraction plane. In Fig. 7, the data were obtained by changing ω and 2θ so as to make traversals between (400) and (420), and between (400) and $(4\bar{2}0)$. The absorption decreased in going from (400) to $(4\bar{2}0)$, and increased in going from (400) to (420). The measured data displayed in Fig. 7 are the average of the data in these two directions corrected for such absorption effects. The data of Fig. 9 have been corrected downward to account for decreased absorption caused by changes in ω.

The [100] data are skewed downward with respect to the calculated points in a direction in each instance which corresponds to increasing 2θ. It definitely has the shape which is predicted, but it is everywhere higher than expected from the calculations. Paskin and Weiss[30] also have measured the TDS from lead in this direction, but their data flatten out at the bottom and do not show the expected rise at the zone boundary. Figures 10 and 11 display the percent excess of the [100] data with respect to that expected from calculations.

In a similar manner the [111] data also are skewed downward with respect to the calculations. Except for a portion of the [111] T data, they are everywhere considerably higher than expected. The [111] L data are very similar in shape to that acquired by Paskin and Weiss, particularly as far as the bump approximately 0.75 units from the (111) reciprocal-lattice point is concerned. This bump is thought by us to be the remnants of a very strong powder

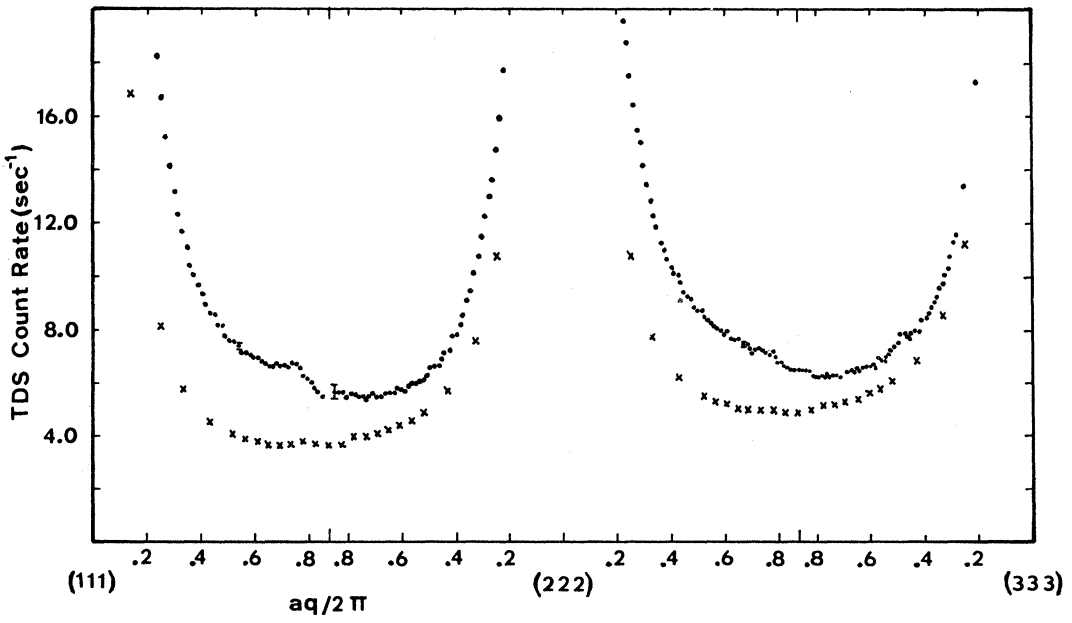

FIG. 8. Total [111] longitudinal TDS. • experimental points; × calculated points.

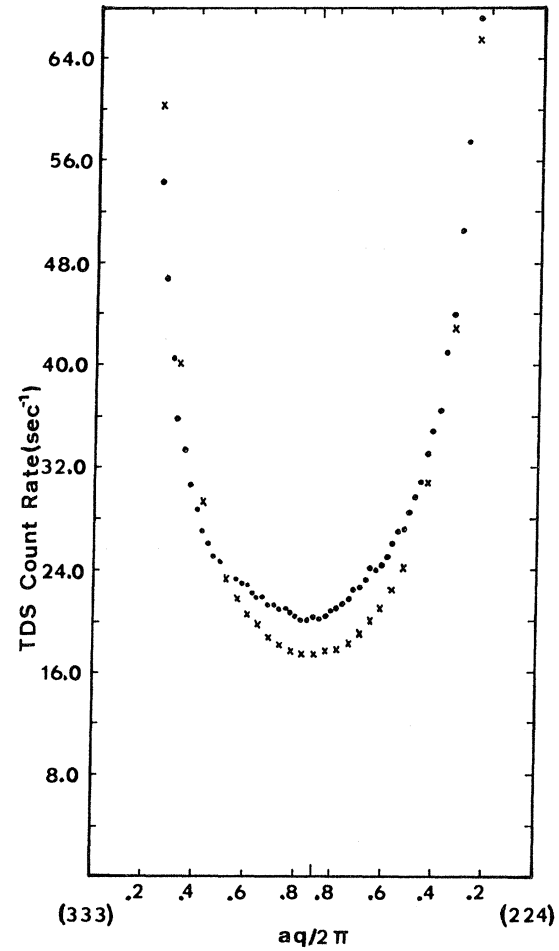

FIG. 9. Total [111] transverse TDS. • experimental points; × calculated points.

peak observed before ion bombardment. Figures 12 and 13 display the percent excess of the [111] data with respect to the calculations.

The most striking feature of these plots is the way in which the measured data are skewed with respect to the calculated points. Although an additive effect was considered, the effect appears to us to be multiplicative in nature, and it has a periodic dependence on reciprocal-lattice position.

V. DISCUSSION

Even though we have used a second-order harmonic calculation, which is exact in the sense that measured force constants have been used, there still is found to be scattering in excess of that expected from the calculations. Several possible sources of this extra scattering are now considered.

Spurious instrumental scatter was not the problem, since with the same experimental system TDS from cesium-iodide single crystals agreed well with that expected from calculations.[18] In addition, the shape of the scattering in the [111] direction has been found to be the same with other experimental arrangements.[30, 31]

The atomic scattering factor[21] and the associated dispersion correction[22] used should be quite good for lead, since relativistic and exchange effects were used in their calculation. The scattering factor used was that for a rigid un-ionized free atom. Since in lead the outer three electrons are considered to be conduction electrons, the scattering factor for Pb^{+3} would have been a better choice. However, calculations of the Pb^{+2} and Pb^{+4} atomic scattering factors[20] indicate that the difference between the Pb and Pb^{+3} scattering factors is negli-

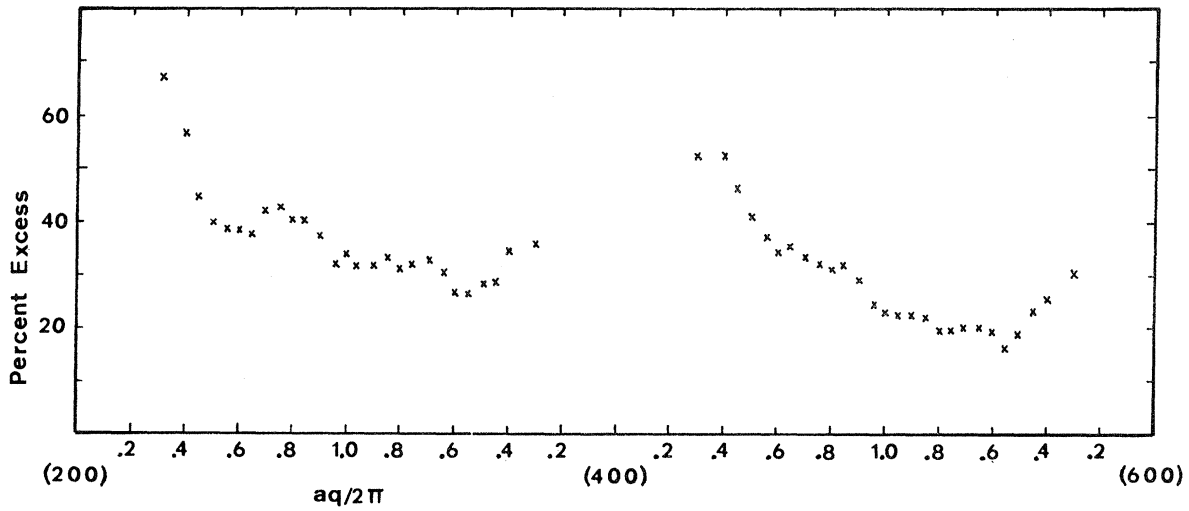

FIG. 10. Percent excess of the [100] longitudinal data with respect to calculations.

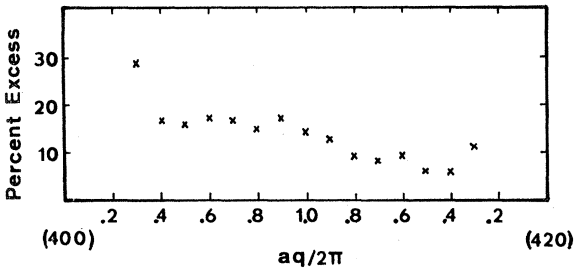

FIG. 11. Percent excess of the [100] transverse data with respect to calculations.

gible for the regions of reciprocal space traversed. Although they are everywhere positive, the periodic variations in the percent differences are similar in shape to those observed in the alkali halides.[32] These variations have been explained in part by effects on the scattering factor which arise from considering an ion to be deformable instead of rigid. This may play a role in the present case.

The Debye-Waller factor and the B and k values do not seem to be the source of the difference. Several sample calculations for the [111] L and [100] L data have been made using Debye-Waller factors corresponding to Debye temperatures of 91 and 79 °K. These calculations varied from the 85 °K calculations by only about 2%. The B and k values, which were determined by scattering from lucite, do not differ much from those obtained in one trial run with paraffin. The paraffin B value was about 1.3% higher than the lucite value, while the paraffin k value was about 6% lower. When the paraffin B and k values were used in calculations in the [111] direction, there was little difference between these calculations and those in which the lucite values were used, particularly between the (111) and (222) reciprocal-lattice points, where the difference between experiment and calculation is the largest. In addition, the Debye-Waller factor and the polarization factor vary smoothly with 2θ, and thus could not contribute to the periodic character of the excess scattering.

There is some uncertainty in the second-order calculation because the phonon frequency distribution calculated by Gilat[14] with the force constants employed here does not agree well with that measured experimentally by Stedman *et al.*[33] This means that the force constants, determined from the fit of symmetry-direction frequencies, do not yield the correct frequencies and polarization vectors in nonsymmetry directions. Since the nonsymmetry directions were summed over in the second-order calculation, there was probably some error introduced. However, in addition to having its magnitude increased, the second-order calculation would have to be skewed considerably in order to account for the differences between calculation and measurements. The second-order calculation cannot be skewed anymore than it is, at least in the [111] L and [100] L calculations, for the integral involved is symmetric with respect to a Brillouin zone boundary in these directions. Any skewness depends only on the factors which multiply the integral. Thus, even though the use of correct fre-

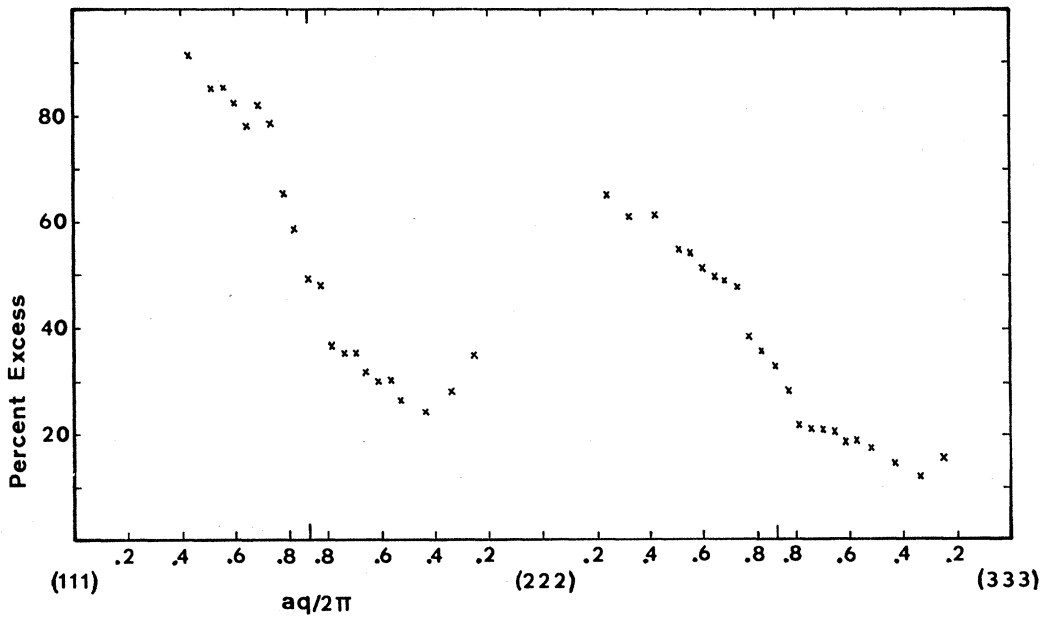

FIG. 12. Percent excess of the [111] longitudinal data with respect to calculations.

quencies and polarization vectors everywhere might change the magnitude of the calculation, the skewness could not be accounted for.

There was also concern that the use of the 100 °K force constants would bring an error into the calculation, but a rough estimate of the change expected in the second-order TDS due to the use of room-temperature constants indicated that the change is probably negligible. To estimate this effect, the 100 °K dispersion curves for lead determined by Stedman *et al.*[2] were compared with the corresponding data acquired at room temperature. The average percentage shift from the values at 100 °K for all frequencies determined at room temperature was about – 4%. For a simple linear restoring force, the percent change in the force constant is twice the percent change in the frequency. In order to make a rough calculation, it was then assumed that each of the atomic force constants determined by Gilat[14] is reduced in magnitude by 8% at room temperature. The effect on the calculated total scattering of using the reduced force constants in the second-order calculation was a change in the correct direction, but one which was very small with respect to the difference between measured data and calculations.

The higher-order scattering calculation is not the problem; if it were, the difference between the calculation and measurement should decrease as one moves toward the reciprocal-space origin.

Various types of surface effects may be involved in this problem. The frequencies of surface waves should be different from those of the bulk waves. Gazis *et al.*,[34] and more recently Allen *et al.*,[35] have investigated surface elastic waves, and Wallis and Maradudin[36] have developed a theory concerning surface wave effects on the TDS from crystal lattices. However, the latter have found no way to separate the surface-phonon from the bulk-phonon contribution to the TDS. Although cesium has a large mass-absorption coefficient, measurements in this laboratory of TDS from cesium iodide[18] indicate that surface phonons contribute very little to the total TDS. This may also be the case with lead. Another surface effect is that due to any residual surface oxides and the sputtered carbon layer. Although there may be some Kohn anomalies among them, most of the small bumps in the measured data are remnants of powder peaks. Diffuse scattering from surface oxides and an amorphous carbon layer would be present to some extent, but it certainly could not explain the periodic character of the extra scattering. This periodic character also cannot be explained by absorption effects arising from an irregular crystal surface. In the case of random roughness, one would expect the effect of the roughness to average out. In addition, if an absorption effect were the problem, the percent difference between measurements and calculations should decrease smoothly, instead of showing the periodic characteristic, as one moves away from the origin of reciprocal space.

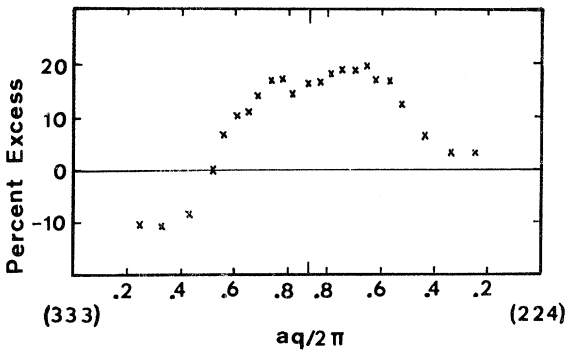

FIG. 13. Percent excess of the [111] transverse data with respect to calculations.

Divergence effects do not seem to be the problem. Rough calculations have indicated that angular divergences much larger than those employed in this work would be necessary to account for the magnitude of the difference between experiment and calculation. In addition, the work on cesium iodide,[18] which was carried out on the same apparatus with the same divergence conditions, indicates that only small divergence corrections are necessary, and only near reciprocal-lattice points.

Recent work by Cowley *et al.*[37] indicates that anharmonic effects cannot be neglected in the calculation of the TDS. Such effects in alkali halides have a form similar to that of the TDS from lead, but instead of being positive nearly everywhere, the differences usually are negative once the zone boundary has been passed. Anharmonic effects were neglected in the present calculations, and these might at least skew the calculations in the correct direction. However, it is unknown whether they would give the necessary increase in the magnitude of the calculated intensities.

In summary, the above considerations do not pinpoint a source for the observed extra scattering. The periodic variations in reciprocal space of the percent difference between the measurements and calculations may be due to the effect of deformable ions on the atomic scattering factor. They could also be due to the neglect of anharmonic effects in the calculation of the TDS. The magnitude of the extra scattering might be connected with the second-order calculation, even though this calculation displays the characteristics expected of it. Scattering from the amorphous carbon layer and small amounts of surface oxides probably gives a little extra scattering, but it does not explain the periodic character of the scattering. The other ef-

fects considered are thought to be negligible.

ACKNOWLEDGMENTS

The authors wish to acknowledge the assistance of P. Schulze, J. Beaver, and E. Brooks, and the valuable advice of Dr. J. Costello and Dr. J. Eldridge.

---

*Work supported by the U. S. Atomic Energy Commission.

†Based on a Ph. D. thesis of S. L. Schuster at the University of Nebraska, Lincoln, Neb. 68508.

[1]B. N. Brockhouse, T. Arase, G. Caglioti, K. R. Rao, and A. D. B. Woods, Phys. Rev. 128, 1099 (1962).

[2]R. Stedman, L. Almquist, G. Nilsson, and G. Raunio, Phys. Rev. 162, 545 (1967).

[3]P. Olmer, Bull. Soc. Franc. Mineral Crist. 71, 145 (1948); Acta Cryst. 1, 57 (1948).

[4]H. Curien, Bull. Soc. Franc. Mineral Crist. 75, 343 (1952); Acta Cryst. 5, 392 (1952).

[5]R. E. Joynson, Phys. Rev. 94, 851 (1954).

[6]E. H. Jacobsen, Phys. Rev. 97, 654 (1955).

[7]C. B. Walker, Phys. Rev. 103, 547 (1956).

[8]S. V. Semenovskaya, Y. S. Umanskii, I. M. Ruzei, and E. B. Granovskii, Fiz. Tverd. Tela 6, 1100 (1964) [Sov. Phys. Solid State 6, 848 (1964)].

[9]R. Stedman and G. Nilsson, Phys. Rev. 145, 492 (1966).

[10]*International Tables for X-Ray Crystallography* (Kynoch, Birmingham, England, 1962), Vol. III.

[11]R. W. James, *The Optical Principles of the Diffraction of X-Rays* (Cornell U. P., Ithaca, N. Y., 1965), Chap. V.

[12]B. N. Brockhouse, T. Arase, G. Caglioti, M. Sakamoto, R. N. Sinclair, and A. D. B. Woods, *Inelastic Scattering of Neutrons in Solids and Liquids* (International Atomic Energy Agency, Vienna, 1961), p. 531.

[13]Nanny Nilsson-Froman, Arkiv Fysik 16, 329 (1959).

[14]G. Gilat, Solid State Commun. 3, 101 (1965).

[15]S. Schuster, Ph. D. thesis (University of Nebraska, 1969) (unpublished).

[16]G. L. Squires, Arkiv Fysik 26, 223 (1964).

[17]J. E. Eldridge and T. R. Lomer, Proc. Phys. Soc. (London) 91, 459 (1967).

[18]J. E. Eldridge, J. Phys. C 3, 1527 (1970).

[19]Reference 11, p. 23.

[20]W. Heisenberg, Z. Physik 32, 737 (1932).

[21]D. Cromer and J. Waber, Acta Cryst. 18, 104 (1965).

[22]D. Cromer, Act Cryst. 18, 17 (1965).

[23]K. Alexopoulos, J. Boskovits, S. Maurikis, and M. Roilas, Acta Cryst. 19, 349 (1965).

[24]S. Schuster, Ph. D. thesis (University of Nebraska, 1969) (unpublished).

[25]B. E. Warren, J. Appl. Phys. 25, 814 (1954).

[26]D. R. Chipman, Rev. Sci. Instr. 27, 164 (1956).

[27]J. M. Costello and J. W. Weymouth, Phys. Rev. 184, 694 (1969).

[28]J. W. Weymouth, J. Costello, S. Schuster, and P. Schulze, Rev. Sci. Instr. 39, 476 (1968).

[29]L. D. Jennings, Acta Cryst. A24, 472 (1968).

[30]A. Paskin and R. J. Weiss, Phys. Rev. Letters 9, 199 (1962).

[31]J. Costello (private communication).

[32]W. Buyers, J. Pirie, and T. Smith, Phys. Rev. 165, 999 (1968).

[33]R. Stedman, L. Almquist, and G. Nilsson, Phys. Rev. 162, 549 (1967).

[34]D. Gazis, R. Herman, and R. Wallis, Phys. Rev. 119, 533 (1960).

[35]R. E. Allen, G. P. Alldredge, and F. W. deWette, Phys. Rev. Letters 23, 1285 (1969).

[36]R. Wallis and A. Maradudin, Phys. Rev. 148, 962 (1966).

[37]R. A. Cowley, E. C. Svensson, and W. J. L. Buyers, Phys. Rev. Letters 23, 525 (1969).